Comparison of COP estimation methods for large-scale heat pumps used in energy planning

Pieper, Henrik; Ommen, Torben; Jensen, Jonas Kjær; Elmegaard, Brian; Markussen, Wiebke Brix

Published in:
Energy

Link to article, DOI:
10.1016/j.energy.2020.117994

Publication date:
2020

Document Version
Peer reviewed version

Comparison of COP estimation methods for large-scale heat pumps used in energy planning

Henrik Pieper[a,*], Torben Ommen[b], Jonas Kjær Jensen[b], Brian Elmegaard[b] and Wiebke Brix Markussen[b]

[a] Tallinn University of Technology, Department of Energy Technology, Ehitajate tee 5, 19086 Tallinn, Estonia
[b] Technical University of Denmark, Department of Mechanical Engineering, Nils Koppels Allé Building 403, 2800 Kgs. Lyngby, Denmark

Abstract

This paper compares estimation of the coefficient of performance (COP) of a large-scale heat pump (HP) for district heating based on four methods to the COP obtained using a detailed thermodynamic HP model. Four heat sources and varying district heating supply temperatures were considered. The COP estimation methods are based on constant COP, Lorenz efficiency, exergy efficiency and a method presented by Jensen et al. (2018). They were implemented in an energy planning tool and further analysed. The planning tool was used to assess HP implementation in a new district in Copenhagen, Denmark. The change in seasonal COP of the HPs, the economic results and optimal HP capacities were compared.

The results show that the Jensen et al. (2018) method provides good approximations and that the planning tool identifies a similar solution compared to the use of the thermodynamic HP model. Assuming a constant Lorenz efficiency, exergy efficiency or COP over the year resulted in large deviations in COP, especially for operations very different from the design conditions. Consequently, other heat sources were found for the most economical solution. The accuracy of the three methods decreased when the initial assumptions of constant COP and efficiencies differed from the ones at design conditions.

Keywords:

COP estimation, District heating, Energy planning, Large-scale heat pumps, Low-temperature heat sources.

1. Introduction

Large-scale heat pumps (HPs) are proposed as a technology for future energy systems to help integrate a high share of renewable electricity production, such as wind power or solar power, into the energy system by coupling the power and district heating (DH) sectors [1,2]. In 2014, the Danish Energy Agency estimated 1050 MW of large-scale HPs installed in Denmark for a high wind scenario of 2050 [3]. Another study estimated that 2450 MW of large-scale HPs supplying DH would have to be installed for the future energy system in 2050 [4]. Currently, 75 MW of such HPs have been

* Corresponding author
Email addresses: henrik.pieper@taltech.ee (Henrik Pieper), tsom@mek.dtu.dk (Torben Ommen), jkjje@mek.dtu.dk (Jonas Kjær Jensen), be@mek.dtu.dk (Brian Elmegaard), wb@mek.dtu.dk (Wiebke Brix Markussen)

installed in Denmark [5]. For Europe, David et al. [15] identified 149 existing large-scale HPs with a thermal capacity above 1 MW supplying DH.

Energy planning tools are often used to investigate the most economic and/or sustainable supply of energy, in form of heat or electricity, for a country, region, city or new development district. In such tools, HPs are often represented in a simplified way to solve the optimization problem faster than if a thermodynamic HP model was included. Lund et al. [6] used the energy planning tools EnergyPlan [7] and MODEST [8] for their analysis of integrating large-scale HPs in Denmark. They assumed a constant coefficient of performance (COP) of the HPs. A range of other studies also assumed a simplified constant COP. Hedegaard and Balyk [9] looked at the efficient integration of a large share of wind energy into the Danish Energy System of 2030 using individual HPs and hot water storage. Rinne and Syri [10] performed a life cycle assessment study to calculate CO_2 emissions from HPs and combined heat and power (CHP) production in Finland. Luickx et al. [11] focused on the impact of the power generation and CO_2 emissions in Belgium when integrating large amounts of HPs. Mathiesen and Lund [12] used EnergyPlan [7] to compare how suitable several technologies are to integrate fluctuating wind power in the energy system. One of those technologies were large-scale HPs.

Because the HP performance is highly dependent on ambient conditions, the constant COP may not represent the real implementation well. Other studies have included variation in one or more temperature levels by assuming simple representations of COP based on a Carnot or a Lorenz cycle. An example of this is to relate the COP to an ideal Lorenz cycle, multiplied by a constant Lorenz efficiency. This allows seasonal changes of inlet and outlet temperatures of the heat source and heat sink to be taken into account. Examples of this practise are Lund et al. [13] and Østergaard and Andersen [14], who used the energy planning tools EnergyPlan [7] and energyPRO [15], respectively.

Several studies show how the COP may be calculated or estimated based on different approaches. Jensen et al. [16] derived an equation for COP based on exergy efficiency, considering the heat source and sink stream temperatures above the dead state. Oluleye et al. [17] and Oluleye et al. [18] derived linear correlations of the Carnot efficiency of a HP for six different refrigerants. Coefficients were provided for condensing temperatures above 50 °C and evaporation temperatures above 10 °C. Jensen et al. [19] derived a generic equation to estimate the COP of a one-stage HP cycle in design conditions. The estimation depends on the heat source and heat sink temperatures as well as on characteristics of the compressor, heat exchangers and the refrigerant integration with the hot and cold stream. This work was further expanded by Ommen et al. [20] by estimating the COP of HPs for operations different from design conditions. Their estimations are based on two validated thermodynamic HP models that represent real HP installations.

The literature survey showed that different COP estimation methods have been implemented in energy planning tools. If these estimations represent HP performance well enough was not assessed. Furthermore, the impact of COP estimations on the model results of energy planning tools were not addressed. Therefore, this study aims at analysing various COP estimation methods by

- Comparing and analysing COP estimation methods to the COP calculated by a thermodynamic HP model for different heat sources.
- Comparing and analysing the model results of an energy planning model for the use of different COP estimation methods and the COPs calculated with a thermodynamic HP model.

2. Method

Four COP estimations were compared to a thermodynamic HP model by calculating the hourly COP based on four different heat sources over one year. Furthermore, the different COP estimation methods were implemented in an energy planning model, which was used for investigating possibilities of installing large-scale HPs to supply DH to a development region in Copenhagen, Denmark. The model is based on mixed-integer linear programming and identified the most economical HP capacities depending on the heat source. Ambient air, groundwater, sewage water and seawater were considered as heat sources for this area.

First, the development of a thermodynamic HP model is presented for design and off-design conditions. The thermodynamic HP model serves as an example of adding additional details to the evaluation of COP in energy planning. Then, the four different COP estimation methods are described, followed by a description of the energy planning tool, the case study and considered heat sources.

2.1. Thermodynamic HP model

A thermodynamic HP model was developed in the software Engineering Equation Solver (EES), version 10.478 [21] considering the different state points of the heat pumping process, as shown in Figure 1.

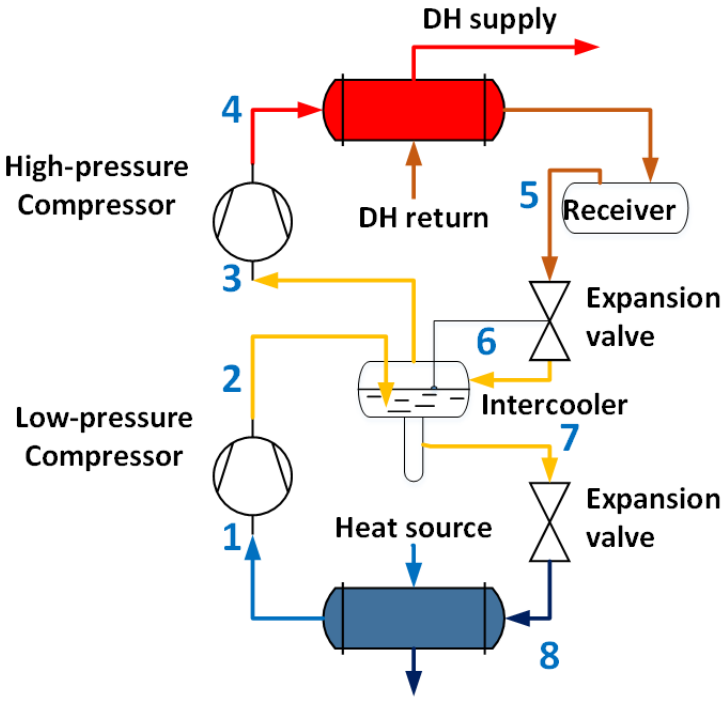

Figure 1. PI-diagram of two-stage HP cycle

The two-stage HP with open intercooler ensures lower pressure ratios and lower discharge temperature out of the compressor, compared to a single-stage HP cycle. Ammonia was chosen as refrigerant, because it has neither global warming nor ozone depletion potential [22]. Two-stage HPs with ammonia as refrigerant have been widely used in DH [23]. First, a HP model was developed for dimensioning the HP in design conditions. Afterwards, the dimensioning parameters were used as inputs to a HP model for off-design conditions, in which the temperatures of heat source and heat sink were varied.

2.1.1. HP design model

The thermodynamic HP model is based on mass and energy balances for all the components. In the design model the dimensioning temperatures were used as input in order to calculate the thermal conductance, i.e., UA-values, of the evaporator and condenser units. The dimensioning capacity was used to calculate the needed displacement rate of the compressors for design conditions, as specified in Table 1. The compressors were assumed to be screw compressors. The heat exchangers were modelled as counter-flow configuration. The heat transfer process in the condenser unit was modelled as three parts consisting of de-superheating, condensing and sub-cooling, each satisfying the energy balances between the refrigerant of the HP and the DH water. A dimensioning heating capacity of 80 % of the hourly peak heat demand for the case study was assumed. Compressor heat loss was neglected.

Table 1. Design conditions for HP dimensioning

Parameter	Value	Unit	Parameter	Value	Unit
Heating capacity	16	MW	Air inlet temperature	−12	°C
DH Supply/return temperature	85/35	°C	Seawater inlet temperature	4	°C
Superheat	0	K	Groundwater inlet temperature	10	°C
Compressor heat loss	0	-	Sewage water inlet temperature	11	°C
Built-in volume ratio	2.2	-	Heat source design temperature difference	6	K
Isentropic design efficiency, $\eta_{is,max}$	0.80	-	Seawater design temperature difference	3	K
Volumetric efficiency	0.90	-	Pinch point design temperature differences	5	K

The isentropic efficiency of the compressors was modelled by a relation developed for screw compressors [22], which takes into account the pressure ratio (p_{HP}/p_{LP}), the built-in pressure ratio ($\pi = v^{\kappa}$), with the built-in volume ratio, v, and the polytropic exponent κ, as shown in Eq. (1). Thereby, losses due to the mismatch between the built-in pressure ratio and the actual pressure ratio were considered. The built in volume ratio was optimized to maximize the isentropic efficiency at design conditions.

$$\eta_{is} = \eta_{is,max} \frac{(p_{HP}/p_{LP})^{(\kappa-1)/\kappa} - 1}{\pi^{(\kappa-1)/\kappa} - \frac{\kappa-1}{\kappa}\pi^{-(1/\kappa)}(\pi - p_{HP}/p_{LP}) - 1} \quad (1)$$

The intermediate pressure was optimized for design conditions to maximize COP. An overview of the modelled HP cycle for design conditions and sewage water as the heat source is shown in Figure 2 as a temperature-heat load (T-$\dot{Q}$) diagram (*a*) and a pressure-enthalpy (p-h) diagram (*b*). The de-superheating (DSH), condensing (Cond) and sub-cooling (SC) part as well as the pinch point temperature difference (PP), DH supply (DH_s) and return (DH_r) temperature and state points are indicated. The refrigerant was sub-cooled by the DH return temperature down to a temperature difference of 5 K.

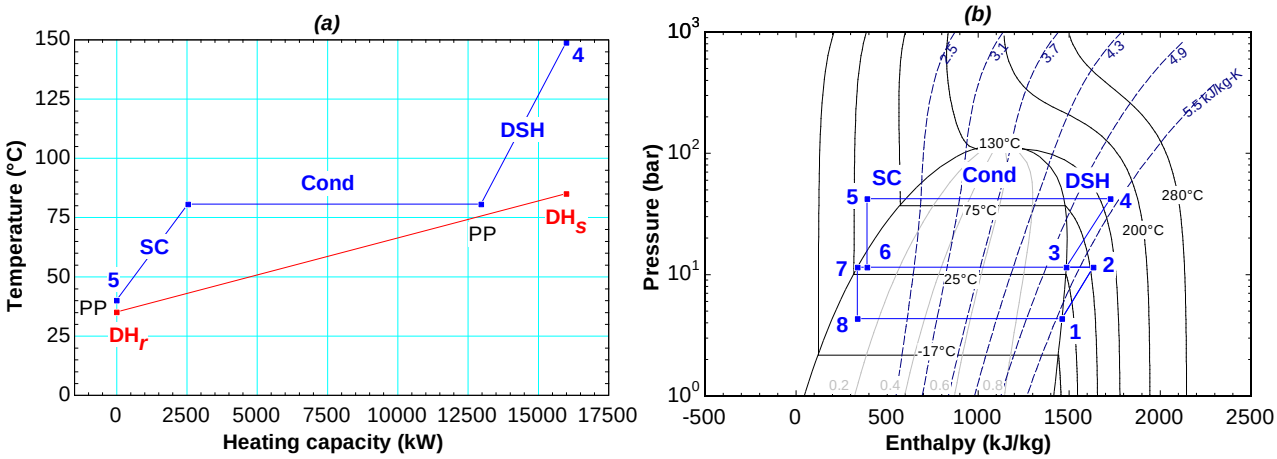

Figure 2. T-$\dot{Q}$ diagram (a) and p-h diagram (b) for HP cycle using sewage water as heat source

2.1.2. HP off-design model

The HP model was modified to allow calculations in off-design conditions. The low-pressure and high-pressure compressor speed (rpm) were synchronized for variations in heat source and heat sink temperature. Part-load behaviour was not considered in the assessment and thus not further addressed. In off-design, the isentropic efficiency of the compressor varied according to Eq. (1). Furthermore,

the UA-values of the evaporator, the sum of the UA-values of the condenser unit (DSH, Cond, SC) and the displacement rates of the compressors were assumed constant. Instead, the intermediate pressure, the condensing temperature and the evaporation temperature were free variables. These three variables were determined according to the change in heat source and heat sink temperatures.

2.1.3. Considerations for HPs with large seasonal variation in heat source temperature

The pressure ratios changed considerably over the year for HPs that use a heat source with large temperature variations during the year. This is the case for using ambient air as the heat source. This would result in very low isentropic efficiencies of the compressor during summer periods, when the pressure ratio decreases below the one at design conditions, as shown in Figure 3 for a polytrophic exponent of 1.5 for ammonia and a built-in volume ratio of 2.8. A different control or design may be chosen for this case and therefore, the relation from Eq. (1) was not used for the air-source HP at all. Instead, a constant isentropic efficiency of 0.80 was assumed representing a best-case scenario.

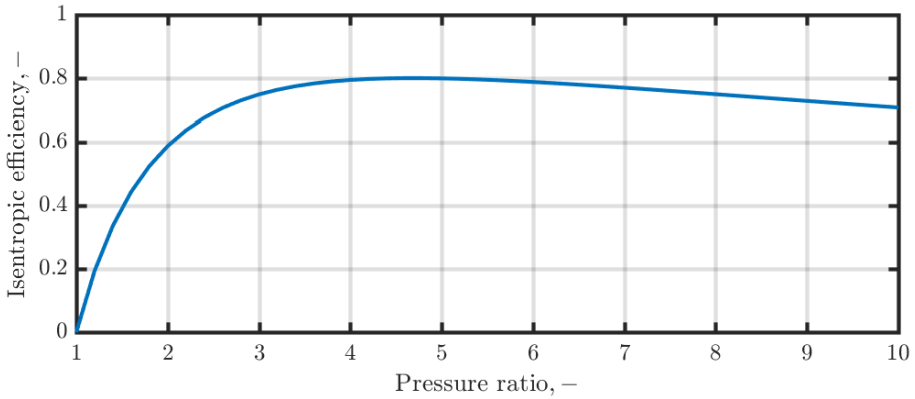

Figure 3. Isentropic efficiency of the compressor as a function of the pressure ratio

2.2. COP estimation methods

Four COP estimation methods are described in the following. The results of the thermodynamic model were used for the design parameters of the COP estimation methods. This was done to allow a fair comparison of the different estimation methods and to the thermodynamic HP model. If such model was not available, guesses had to be made for parameters required for the COP estimations. These would have to be based on reference values found in literature or from suppliers. Those values could differ considerably from those found using the thermodynamic model.

2.2.1. Constant COP

The COPs calculated for the different heat sources based on the thermodynamic HP model for design conditions were used as the constant COPs for the entire year.

2.2.2. Constant Lorenz efficiency

This estimation was based on the COP of a Lorenz cycle which was multiplied by a constant Lorenz efficiency, as shown in Eq. (2). The Lorenz cycle COP is based on the logarithmic mean temperatures of the heat sink and heat source, as shown in Eq. (3). The constant value of the Lorenz efficiency was determined based on the design conditions of the thermodynamic model.

$$\mathrm{COP}_\eta = \eta_{L,m}\mathrm{COP}_L = \eta_{L,m}\frac{\bar{T}_H}{\bar{T}_H - \bar{T}_C} \tag{2}$$

$$\bar{T}_H = \frac{T_{H,o} - T_{H,i}}{\ln\left(\frac{T_{H,o}}{T_{H,i}}\right)}, \quad \bar{T}_C = \frac{T_{C,i} - T_{C,o}}{\ln\left(\frac{T_{C,i}}{T_{C,o}}\right)} \tag{3}$$

2.2.3. Constant exergy efficiency

Exergy efficiency indicates the percentage of exergy recovered in the desired product compared to the exergy supplied to the HP system. The exergy efficiency of the thermodynamic HP model, ε_m, was calculated as the ratio of exergy product and exergy fuel, as shown in Eq. (4). Thermal exergy was the only exergy part considered. It can be expressed for a stream of matter *j*, as shown in Eq. (5).

$$\varepsilon_m = \frac{\dot{E}_P}{\dot{E}_F} \tag{4}$$

$$\dot{E}_j = \dot{m}_j(h_j - h_0) - \dot{m}_j T_0(s_j - s_0) \tag{5}$$

Both the exergy product and the exergy fuel depend on the purpose of the system, its operating conditions and integration into the environment (dead state) [24]. For the HP, the exergy product was considered as the exergy of the supplied heat to the DH network. The exergy fuel was considered as the electrical power for operating the compressor. The dead state temperature, T_0, was set as the heat source inlet temperature during operation. With this assumption the dead state temperature depends on the heat source temperature for each hour during the year. Any contribution of exergy fuel from the heat source below the dead state was neglected. The outlet of the heat source was left unused and thus assumed to be mixed with the ambient. The exergy efficiency for a HP was then calculated as shown in Eq. (6) [16].

$$\varepsilon_m = \frac{\dot{m}_H(h_{H,o} - h_{H,i}) - \dot{m}_H T_0(s_{H,o} - s_{H,i})}{\dot{W}} = \frac{\dot{m}_H c_p(T_{H,o} - T_{H,i}) - T_0 \dot{m}_H c_p \ln\left(\frac{T_{H,o}}{T_{H,i}}\right)}{\dot{W}} \tag{6}$$

The exergy efficiency can be expressed as a function of the Lorenz efficiency, when substituting Eq. (2) and Eq. (3) into Eq. (6), as shown in Eq. (7).

$$\varepsilon_m = \frac{\dot{Q}_H - T_0 \dot{m}_H c_p \ln\left(\frac{T_{H,o}}{T_{H,i}}\right)\frac{(T_{H,o}-T_{H,i})}{(T_{H,o}-T_{H,i})}}{\dot{W}} = \frac{\dot{Q}_H\left(1 - \frac{T_0}{\bar{T}_H}\right)}{\dot{W}} = \eta_{L,m}\frac{\bar{T}_H - T_0}{\bar{T}_H - \bar{T}_C} \tag{7}$$

The COP can be calculated by rearranging Eq. (7), as shown in Eq. (8).

$$\mathrm{COP}_\varepsilon = \frac{\varepsilon_m}{1 - \frac{T_0}{\bar{T}_H}} = \varepsilon_m \frac{\bar{T}_H}{(\bar{T}_H - T_0)} \tag{8}$$

The constant value of the exergy efficiency was determined based on the design conditions of the thermodynamic model. The estimation of COP based on constant exergy efficiency may result in very similar values compared to the case of constant Lorenz efficiency depending on the choice of dead state temperature and temperature difference between the heat source inlet and outlet, as seen by comparing Eq. (2) and Eq. (8).

2.2.4. Jensen et al. COP estimation for design conditions

Another COP estimation method was presented by Jensen et al. [19]. They derived a generic equation for the COP analytically for design conditions of a single-stage HP cycle, as shown in Eq. (9). Even though this method was based on a single-stage HP, it was compared in this study with a two-stage HP model.

$$\mathrm{COP}_J = \left(\mathrm{COP}_L \frac{1 + \frac{\Delta\bar{T}_{r,H} + \Delta\bar{T}_{\mathrm{pp}}}{\bar{T}_H}}{1 + \frac{\Delta\bar{T}_{r,H} + \Delta\bar{T}_{r,C} + 2\Delta\bar{T}_{\mathrm{pp}}}{\bar{T}_H - \bar{T}_C}} \eta_{\mathrm{is},c} \left(1 - \frac{w_{\mathrm{is},e}}{w_{\mathrm{is},c}}\right) + 1 - \eta_{\mathrm{is},c} - f_Q \right) \quad (9)$$

Equation (9) depends only on temperatures of the heat source and heat sink (COP_L, $\bar{T}_H$ and $\bar{T}_C$) as well as characteristics of the compressor (isentropic efficiency $\eta_{\mathrm{is},c}$ and heat loss factor f_Q), the heat exchangers (logarithmic pinch point temperature difference $\Delta\bar{T}_{\mathrm{pp}} \approx \Delta T_{\mathrm{pp}}$) and certain characteristics of the refrigerant ($w_{\mathrm{is},e}/w_{\mathrm{is},c}$, $\Delta\bar{T}_{r,H}$ and $\Delta\bar{T}_{r,C}$). For most of the parameters, reasonable values may be easily assumed. Simple linear approximations are given using ammonia as the refrigerant for $w_{\mathrm{is},e}/w_{\mathrm{is},c}$, $\Delta\bar{T}_{r,H}$ and $\Delta\bar{T}_{r,C}$, which are more difficult to estimate without a thermodynamic HP model. The other input parameters may be found in Table 1 based on design conditions.

2.3. Energy planning model

The optimization model was developed in GAMS, version 24.8.3, [25] with the aim of minimizing total costs including annualised investment costs ($C_{\mathrm{Inv},a}$), annual electricity costs (C_{el}) as well as operation and maintenance (O&M) costs ($C_{\mathrm{O\&M}}$) of each production unit *p*. The optimization was based on mixed-integer linear programming using the CPLEX solver, version 12.7.0.0 [26]. Annual calculations were performed on hourly basis. A more detailed description of the model can be found in Pieper et al. [27]. The objective function is shown in Eq. (10).

$$\min Z = \sum_p Z_p = \sum_p \left(C_{\mathrm{el},p} + C_{\mathrm{O\&M},p} + C_{\mathrm{Inv},a,p}\right) \quad (10)$$

Annualised investment costs were considered, as it was done in [28], to reduce calculation time. They were calculated, as shown in Eq. (11), considering the discount rate, *b*, and lifetime of the plant, *T*. Investment costs of large-scale HPs, depending on the heat source used, were obtained from Pieper et al. [29].

$$C_{\mathrm{Inv},a} = C_{\mathrm{Inv}} \frac{b}{(1+b)(1-(1+b)^{-T})} \quad (11)$$

Short-term storage with a heat loss of 5 % for each hour, *n*, and an electric peak load boiler with COP of 1 were also implemented [30]. The hourly heat demand had to be supplied by the production units and/or the storage, as shown in Eq. (12) and in Figure 4.

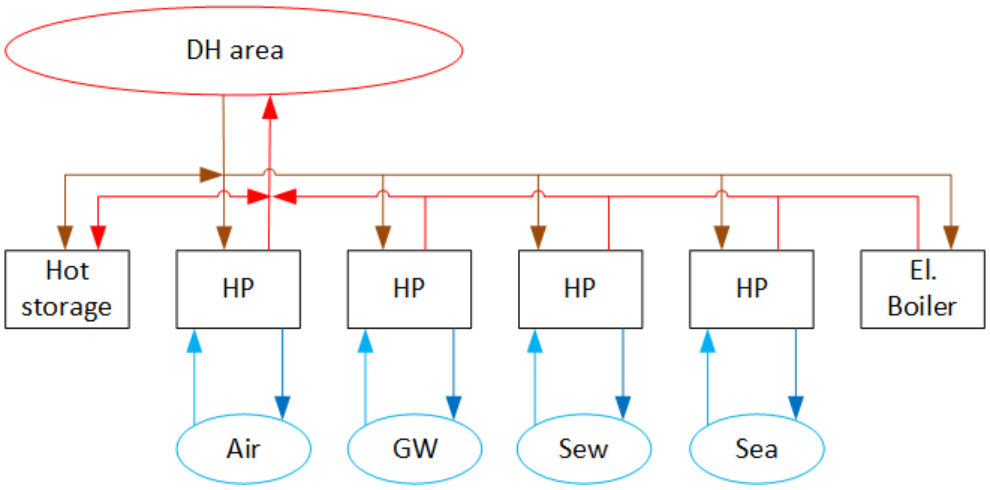

Figure 4. System layout

The model determined the required HP capacity of each heat source, electric boiler capacity and storage capacity by Eq. (13) and Eq. (14), ensuring that the capacities were above the hourly production and storage level, respectively. The storage level of one hour was determined by Eq. (15), considering the storage level of the previous hour, the amount of heat to be stored or discharged and the storage heat loss factor, f_{loss}.

$$\sum_{p} Q_{H,p,n} = Q_{\text{Heat,n}} + Q_{\text{st,char},n} - Q_{\text{st,dis},n} \tag{12}$$

$$\dot{Q}_{H,p} \geq Q_{H,p,n} \tag{13}$$

$$\dot{Q}_{\text{st},c} \geq Q_{\text{st,level},n} \tag{14}$$

$$Q_{\text{st,level},n} = Q_{\text{st,level},n-1} + Q_{\text{st,char},n} - Q_{\text{st,dis},n} - f_{\text{loss}} Q_{\text{st,level},n} \tag{15}$$

The COP of the production units determined the electricity usage and consequently the costs related to that, as shown in Eq. (16).

$$\text{COP}_{p,n} = \frac{Q_{H,p,n}}{P_{p,n}} \tag{16}$$

2.4. Case study

The development district Nordhavn, shown in Figure 5, was used as the case study. This new city district in Copenhagen, Denmark, is surrounded by the sea and will be gradually expanded until 2060 to accommodate 40,000 inhabitants and 40,000 jobs in a floor area of 3.5 million m^2 [31].

Figure 5. Nordhavn area (red) [32]

The relative load duration curve based on hourly measurements from 2018 of the heat demand of the already existing building stock was used as input, as shown in Figure 6. These measurements include heat losses of the existing part of the DH network supplying both commercial and residential buildings. The maximum hourly peak heat demand was assumed to be 20 MW, which resulted in an annual heat demand of 51 GWh.

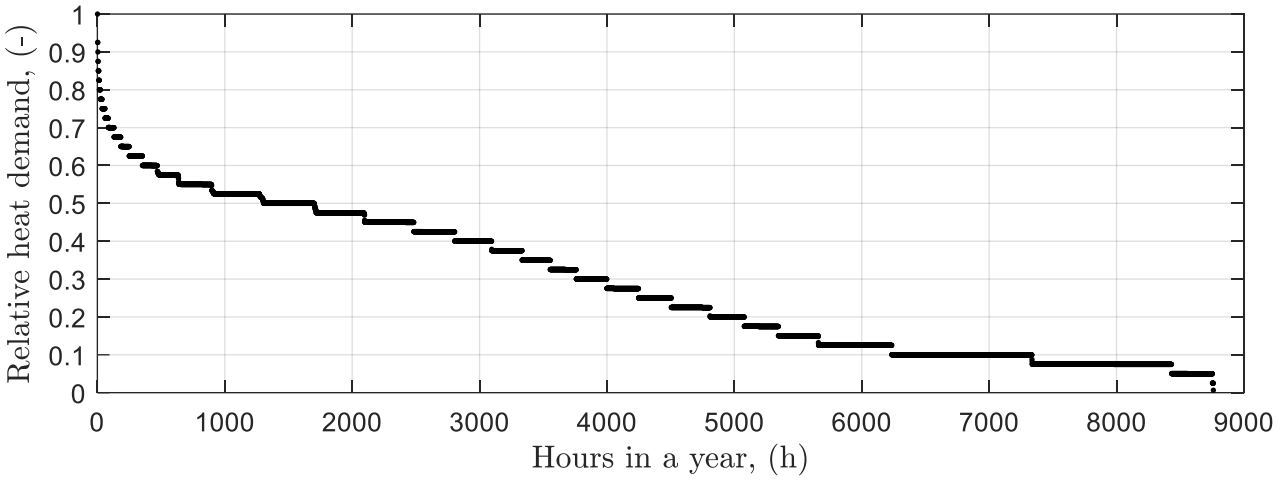

Figure 6. Relative load duration curve for area of Nordhavn (based on data from [33]*)*

A dependency of DH supply temperatures on outdoor temperature T_{amb} was determined in Pieper et al. [34] based on measurements for the area of Nordhavn [35], as shown in Eq. (17). The temperature-dependency was assumed to increase to a maximum of 85 °C during cold periods. This maximum temperature corresponds to the pressure and temperature limitations of state-of-the-art ammonia compressors for HPs [36].

$$T_{H,o,n} = \begin{cases} 70\ °\text{C}, \text{for } T_{\text{amb},n} > 10\ °\text{C} \\ 85\ °\text{C}, \text{for } T_{\text{amb},n} < 2.5\ °\text{C} \\ -2\ T_{\text{amb},n} + 90\ °\text{C}, \text{otherwise} \end{cases} \quad (17)$$

This dependency was further simplified for the sake of clarity of the results, as shown in Figure 7. Constant temperatures were assumed in winter and summer. A linear trend was assumed for April and November. A constant return temperature was assumed at 35 °C.

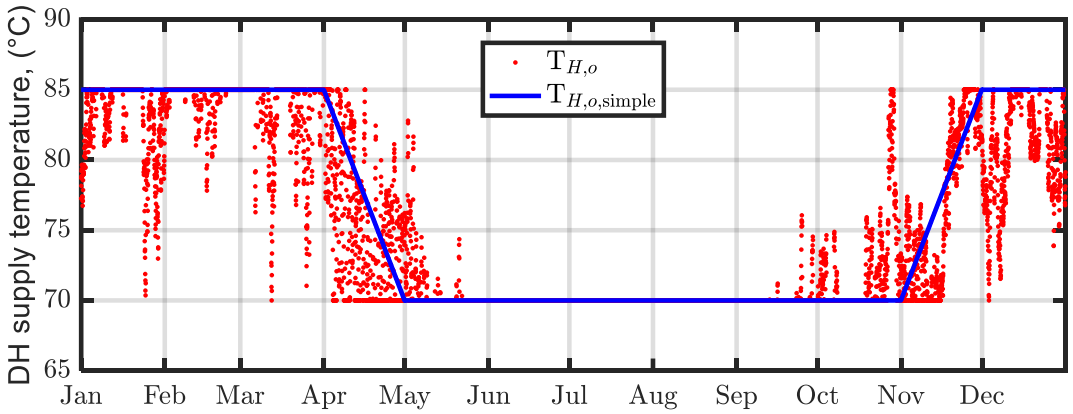

Figure 7. DH supply temperature based on data from [34] *and simplified*

2.4.1. Heat sources

The heat sources considered for this study were ambient air, groundwater, seawater and sewage water. For air, hourly values of the temperature and the relative humidity for the area of Nordhavn were provided for 2018 [37].

The groundwater temperature was assumed to be 10 °C and to be accessed at 100 m depth. Measurements showed a groundwater temperature between 10 °C and 11 °C at this depth and location [38]. This is at the upper end of what is typically found in Denmark (8 °C to 10 °C), which also depends on the depth of the groundwater reservoir [23]. It was assumed that the groundwater HP

capacity was limited to 5 MW due to area constraints. This complies with the largest groundwater HP installations of 4 MW found in Denmark [23]. Such HP capacities require a large amount of groundwater, which is difficult to extract and reinject without compromising the long-term stability. Therefore, the practical limit might be at around 5 MW [39]. An analysis for Nordhavn has shown that pumping 50 m^3/h of water, which may correspond to approximately 0.7 MW HP capacity, influences the groundwater level temporarily by 0.5 m at a distance to the pumping location of approximately 900 m [40]. Thereby, a large area is influenced, which could lead to problems, when more groundwater HPs would be installed in the area nearby. The width of the total area of Nordhavn is around 3 km.

Seawater was assumed to be pumped from 10 m depth, which is the deepest area near the coastline of Nordhavn (distance approximately 200 m). In this way, freezing problems during cold periods can be reduced or avoided, as the temperature in winter is higher at this depth than at the water surface. This is also done for large-scale HPs in Oslo, Norway [41], and in Stockholm, Sweden, [42], however at greater depth compared to Danish conditions. An hourly seawater temperature profile for a depth of 10 m was used [34] based on measurements from 2015 and 2017. The data was provided by the National database (ODA) by the Danish Environmental Protection Agency [43].

Measurements of the daily temperature and volume flow rate of cleaned sewage water were provided for several years for the sewage water treatment plant, Lynetten, located 2 km south from Nordhavn [44]. Cleaned sewage water was preferred over untreated water, because the biological treatment of cleaning the sewage water is sensitive to changes in temperature and thus not to be disturbed [45]. In addition, using untreated water may require additional attention in terms of cleaning equipment and heat exchanger design. Mean values for each day were created based on the different years of available data. The same temperature was assumed for all hours of one day and the daily volume flow rate was evenly distributed for each hour of the day. The hourly volume flow rate varied between 2100 m^3/h and 4350 m^3/h with the mean value being 3035 m^3/h and corresponding to 45 MW HP capacity.

An overview of the hourly temperatures of all considered heat sources may be found in Figure 8.

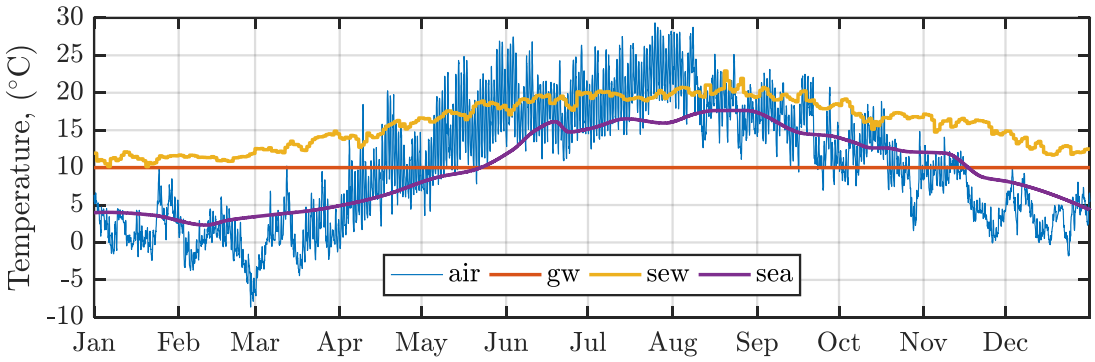

Figure 8. Hourly heat source inlet temperatures of ambient air (air), groundwater (gw), sewage water (sew) and seawater (sea)

2.4.2. Economic input parameters

Hourly electricity prices for the region DK2 were taken from Nord Pool for 2018 [46]. Electricity taxes, system fees and transmission fees were applied. Distribution fees were applied using a weighted mean value of the triple tariff for simplicity [47]. The public service obligation (PSO) was neglected, as it will be phased out by 2022 [48]. Further, the electricity tax will be reduced by 100 DKK/MWh from 2019 if electricity is used to produce heat for DH [49]. Investment costs and O&M costs were obtained from different references. The investment costs were annualised assuming a discount rate of 4 % and a lifetime of piping, the HPs, the storage and electric boilers of 30 years, 25 years, 20 years and 15 years, respectively [50]. Only part of the investment was taken into account for equipment that had a longer lifetime than the HPs. On the contrary, additional investments were

required for the electrical boiler, when needed, due to its shorter lifetime. In case additional DH piping was required to allow the use of certain heat sources, a velocity of 2 m/s was assumed for dimensioning the system. For the case of sewage water, the additional 2 km DH pipe was assumed to correspond to an additional heat loss of 5 %. An overview of the input parameters for variable, investment and O&M cost can be found in Table 2 to Table 4.

Table 2. Electricity costs

Parameter	Value	Unit	Ref.
Nord Pool average price 2018	46.20	€/MWh$_{el}$	[46]
Electricity tax	41.34	€/MWh$_{el}$	[49]
Transmission and system tariff	10.74	€/MWh$_{el}$	[51]
Distribution tariff	13.10	€/MWh$_{el}$	[52]
Total	111.38	€/MWh$_{el}$	

Table 3. Investment costs of DH pipes and storage

Parameter	Investment costs	Unit	Pipe length	Unit	Ref.
DH pipe (sew)	(505+3.1 $\dot{V}_H$)	€/m	2000	m	[53]
DH pipe (sea)	(505+3.1 $\dot{V}_C$)	€/m	200	m	[53]
Storage	205+0.087 V_{st}	T€			[54]

Table 4. Investment costs and O&M costs

Technology	Investments, M€	Ref.	O&M costs, €/MWh	O&M costs, €/MW/a	Ref.
HP (air)	0.183+0.677 $\dot{Q}_H$	[29]	1.0	2000	[23,50]
HP (gw)	0.500+0.640 $\dot{Q}_H$	[29]	2.0	2000	[23,50]
HP (sew)	0.478+0.550 $\dot{Q}_H$	[29]	1.3	2000	[23,50]
HP (sea)	0.478+0.550 $\dot{Q}_H$	[29]	1.3	2000	[23,50]
Electric boiler	0.110 $\dot{Q}_H$	[53]	0.54	1177	[53]

2.5. Performance indicators

The different COP estimation methods were implemented in the energy planning model and the results of the optimizations were compared with each other. Evaluated parameters were the HP capacity for each heat source, the seasonal COP (SCOP) considering storage losses, the levelized costs of heat (LCOH) and the CO_2 emissions per supplied heat based on the electricity consumption of the HPs.

The SCOP takes hourly variations of heat supply Q_n into account by calculating the ratio of the annual supplied heat and the annual consumed electricity, as shown in Eq. (18).

$$\mathrm{SCOP} = \frac{Q_{\mathrm{tot}}}{P_{\mathrm{tot}}} = \frac{\sum_{n=1}^{N} Q_n}{\sum_{n=1}^{N} P_n} \tag{18}$$

The LCOH were calculated as the sum of the heat production costs, including costs for electricity C_{el}, O&M costs ($C_{O\&M}$) and investment costs (C_{Inv}), divided by the annual heat supply, as shown in Eq. (19).

$$\mathrm{LCOH} = \frac{C_{\mathrm{el}} + C_{\mathrm{O\&M}} + C_{\mathrm{Inv}}}{Q_{\mathrm{Heat}}} \tag{19}$$

The CO_2 emissions per unit heat were calculated by the ratio of the annual CO_2 emissions and the annual supply of heating. The annual CO_2 emissions were calculated by multiplying the hourly electricity consumption with the CO_2 emission factor for electricity production for each hour. An

overview of the hourly CO_2 emission factors for the region DK2 for 2018 [55] can be found in Figure 9.

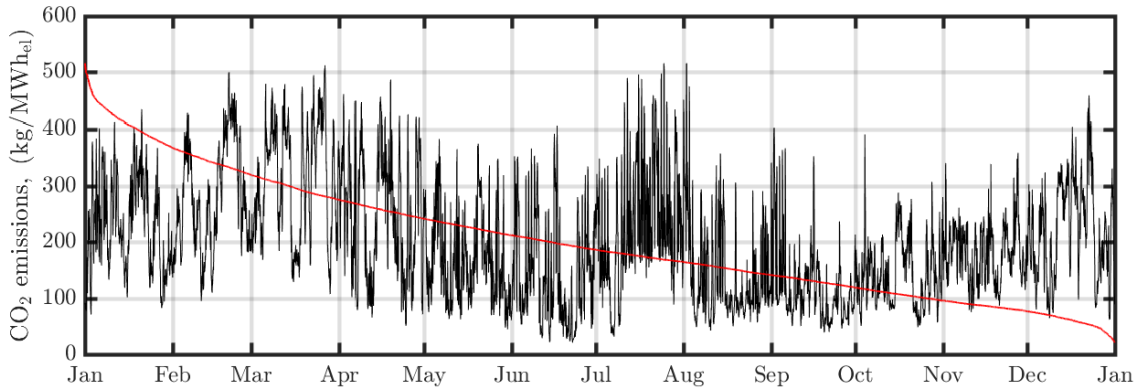

Figure 9. Hourly (black) and sorted (red) CO_2 emissions from electricity production for DK2 for 2018 [55]

2.6. Sensitivity analysis

The COP of the thermodynamic HP model was changed by ±20 % in order to investigate the impact of this change on the LCOH of the optimization results.

The constant COP was changed by ±20 % to show what the impact on the optimization would be, if a different value than the COP based on design conditions was chosen.

For the same reason, the Lorenz efficiency was decreased by 20 %, since it already had high values. Furthermore, the Lorenz efficiency was assumed to be 0.5 equally for all heat sources, which was a value used in literature [13,14].

For the Jensen COP estimation method, the coefficients for the two approximations proposed by Jensen et al. [19] for $w_{\mathrm{is},e}/w_{\mathrm{is},c}$ and $\Delta\bar{T}_{r,H}$ were varied by ±20 %.

3. Results

First, the dimensioning values of the thermodynamic HP model for design conditions are presented. The comparison of COP with the other COP estimation methods follows. Then, the impact of using different COP estimation methods for planning the installation of new HPs and the results of the economic analysis of the energy planning model are presented. Finally, the results of the sensitivity analysis are shown.

3.1. Dimensioning values of thermodynamic HP model

The dimensioning values of the HP design model for the different heat sources are shown in Table 5.

Table 5. Dimensioning values of HP in design conditions

Parameter	Air	GW	Sew	Sea	Unit
COP	2.72	3.42	3.46	3.29	-
Lorenz efficiency	0.61	0.54	0.53	0.56	-
Exergy efficiency	0.58	0.51	0.50	0.55	-
UA_e	1329	1488	1496	1747	kW/K
$UA_{c,\mathrm{tot}}$	878	933	934	929	kW/K
Displacement rates (LP/HP)	6.49/3.21	3.35/1.52	3.25/1.50	3.66/1.60	m^3/s
Pressure ratios (LP/HP)	2.8/8.3	2.7/3.7	2.7/3.7	2.9/3.9	-
Intermediate pressure	4.63	11.24	11.45	10.62	bar

As shown, the COPs were the highest for the heat sources with the highest source temperature. The Lorenz efficiency was higher for lower heat source temperatures. The exergy efficiencies were

slightly below the Lorenz efficiency and higher if the heat source outlet temperature was used as the reference temperature. The optimal intermediate pressure and built-in volume ratio as well as the displacement rates were very different for using ambient air compared to using the three other heat sources, which for these performance indicators were found to be similar in magnitude.

3.2. HP model COPs for different heat sources

The hourly COPs, calculated with the thermodynamic model, for the HPs using the four different heat sources are presented in Figure 10.

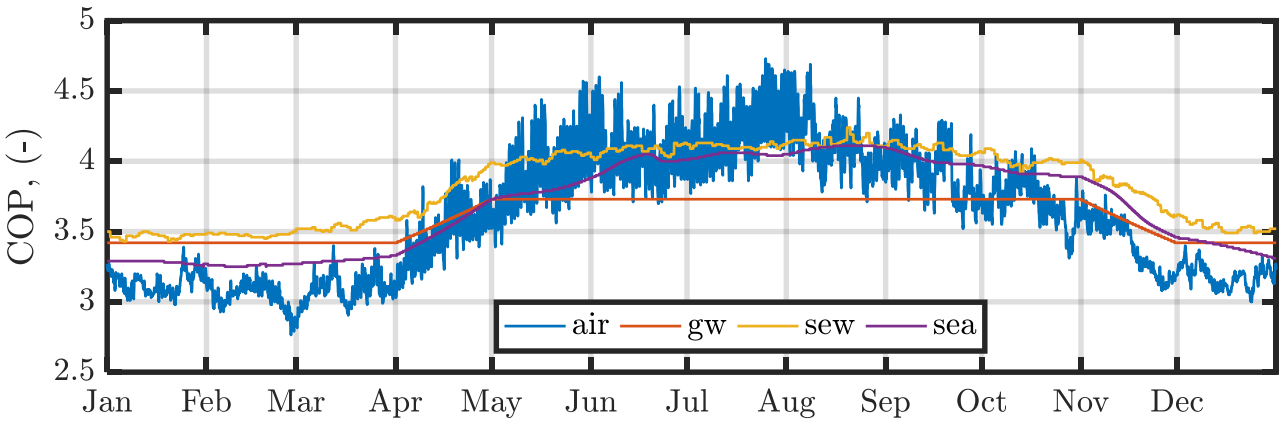

Figure 10. Hourly COPs for HPs calculated with thermodynamic model

As shown, the COPs were generally higher from April to November, due to decreased DH supply temperatures and increased heat source temperatures, apart from groundwater. The COP of the air-source HP fluctuated more during summer, because of the changes in ambient temperature. The COP of the sewage water HP was always higher than for the other water-based HPs. The groundwater HP resulted in higher COPs in winter than the seawater HP. On the contrary, the seawater HP COP was higher during summer, because of the warmer source inlet temperature. The SCOP considering the hourly variations in heat demand of the case study are shown in Table 6.

Table 6: Seasonal COP of HPs based on different heat sources considering the heat demand

Parameter	Air	GW	Sew	Sea	Unit
Seasonal COP	3.30	3.51	3.67	3.48	-

3.3. COP deviations based on different estimation methods

For each hour, the COP of the four different estimation methods was compared to the thermodynamic HP model. The hourly deviations of COP are shown in Figure 11.

For the water-based HPs, each of the four COP estimation methods resulted in very good estimations of COP during winter compared to the thermodynamic model, because the conditions from December until April were very similar to the design conditions. The Jensen estimation method for design conditions (Jensen) underestimated the COP slightly during this period, likely because it was developed for one-stage HP cycles, while a two-stage HP was modelled here. The deviations for the different methods increase during summer when the operating conditions differ considerably from the design conditions.

Using a constant COP based on design conditions resulted in an underestimation of COP of up to −20 % for sewage water and seawater HPs in summer. The deviation was reduced by approximately 50 % for the groundwater HP. However, for the air-source HP, the deviations of the COPs were up to −40 % in summer and −15 % to −20 % in winter. This may be explained by the design conditions, which were set at −12 °C, while the lowest occurring temperature in 2018 for the area of Nordhavn was −8.6 °C.

The COP calculated with the Lorenz method deviates considerably during summer from the one obtained from the thermodynamic model. For the use of ambient air, deviations in COP of 60 % and higher were observed. The deviation would be even larger, because the isentropic efficiency of the compressor at design conditions was used for calculations for the entire year. If sewage water and seawater HPs were used, the COP deviated more than 20 % during some periods. Using a constant Lorenz efficiency throughout the entire year would result in an overestimation of COP for heat sources with seasonal temperature variations. The chosen Lorenz efficiency, based on design conditions, may be too high, since these conditions occur only rarely during the year and because the Lorenz efficiency decreases with smaller temperature lifts, so if the ambient temperature increases and/or the DH temperature decreases.

The COP calculated with a constant exergy efficiency based on the dead state temperature being the heat source inlet temperature resulted in very similar values compared to using the Lorenz method, as described earlier.

The deviations of the Jensen method are below 10 % during summer for all heat sources. The deviations are even lower when the heat source temperature does not vary, as for groundwater. Therefore, the Jensen method gives good approximations of COP throughout the year. In particular, the deviation in summer will have a smaller impact, since the heat demand is typically lower.

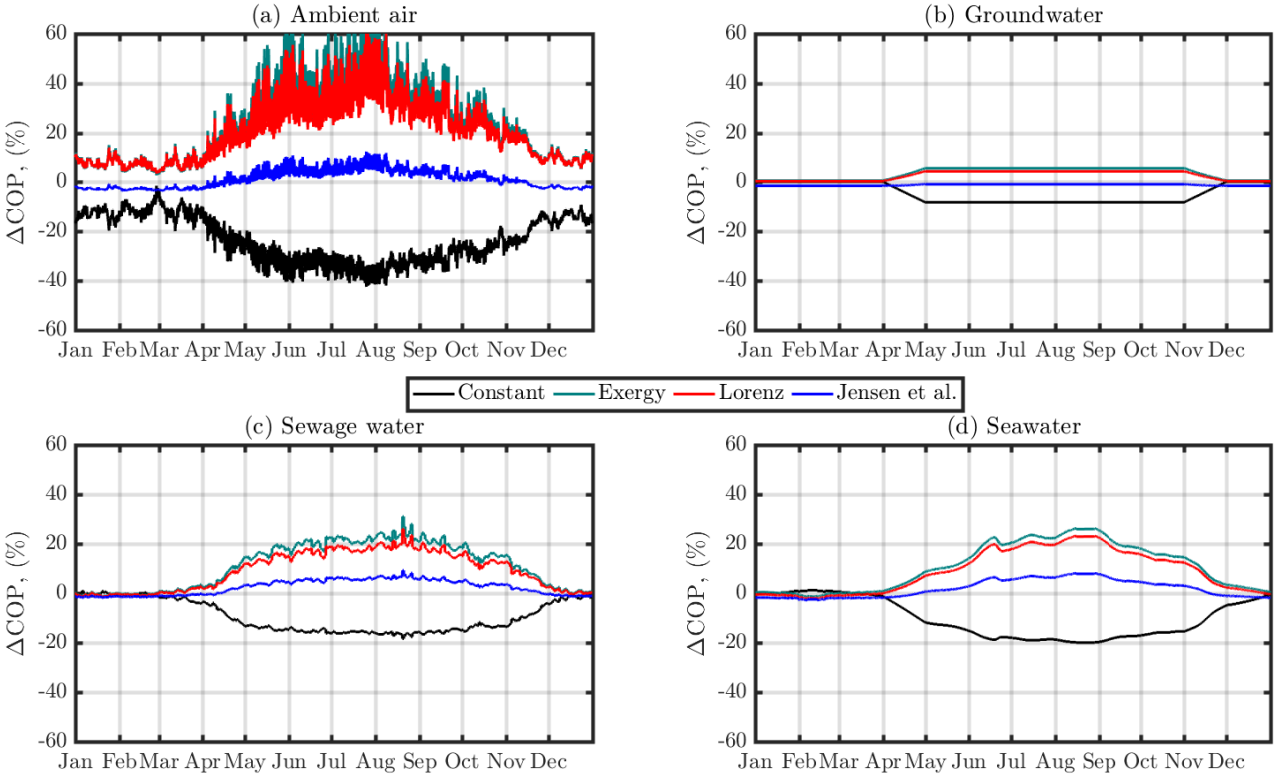

Figure 11. Deviation of COP estimation methods compared to the thermodynamic HP model

3.4. Comparison of optimization results

The results of using the different COP estimation methods in the energy planning tool are found in Table 7 as well as typical values for some of the parameters for installed large-scale HPs supplying DH in Denmark. As shown, using the different estimation methods resulted in a similar total HP capacity of 15.4 MW to 16.1 MW, corresponding to 77 % to 81 % of the hourly peak demand. The remaining load was supplied by discharging the storage, which had sufficient heating capacity, such that no electric boiler would be needed. The hot water storage tank would approximately have a volume of 564 m^3, if completely filled with 85 °C warm water.

Table 7. Results of optimization using different COP estimation methods

Parameter	Thermodynamic Model	Constant	Lorenz/ Exergy	Jensen et al.	Reference [23]
Heat source	Sea	Sea/GW	Air/GW	Sea	
HP capacity, MW	15.4	10.4/5.0	11.1/5.0	15.4	
Storage capacity, MWh	32.2	32.2	28.4	32.2	
Seasonal COP, -	3.4	3.3	3.7	3.4	3.5 to 4.5
LCOH, €/MWh_h	45.2	46.9	44.0	45.3	42 to 49
Electricity, O&M costs, €/MWh_h	31.7	32.9	29.7	31.8	25 to 32
CO_2 emissions, $kgCO_2/MWh_h$	67.0	68.3	63.4	67.6	

The selected heat source depended on the COP estimation method. A 10.4 MW seawater HP and a 5.0 MW groundwater HP was the optimal choice based on the constant COP method. Groundwater was chosen besides seawater, because the method overestimated the HP performance for this heat source during summer. Using the Lorenz method for determining COP resulted in the use of a 11.1 MW air-source HP and a 5.0 MW groundwater HP. The choice for air in this case originated from the large overestimation of COP. Using the Jensen method resulted in the same selection of heat source (seawater) as if the COP was calculated using the thermodynamic model.

The SCOP was very similar for most of the estimation methods, since the overestimation during summer was less significant when the low heat load was considered. The Lorenz method was an exception, which resulted in a high SCOP of 3.7.

The difference in COP is reflected in the economic parameters, e.g. the LCOH was higher when the Constant COP method with lower COPs was used and lower when the Lorenz method was used having higher COPs. A difference in LCOH of 1 €/MWh_h would be a loss or gain of 51,000 € for the 51 GWh annual heat supply. The impact on the economic parameters could be even larger, if the chosen efficiencies and COPs would have been determined without the use of the thermodynamic model. The difference in LCOH for the Jensen et al. method is small.

The CO_2 emissions were 67.0 $kgCO_2/MWh_h$ if the COPs calculated with the thermodynamic model were used as inputs. Using the Jensen et al. COP estimation method resulted in similar CO_2 emissions of 67.6 $kgCO_2/MWh_h$. The emissions were 1.3 $kgCO_2/MWh_h$ larger for the case of using a constant COP. The results of the optimization when the Lorenz method was used lead to 3.6 $kgCO_2/MWh_h$ lower CO_2 emissions than the solutions obtained using the COPs obtained from the thermodynamic model. The calculated annual CO_2 emissions would be 184 t lower than the ones based on the optimization using COPs calculated with the thermodynamic model.

3.5. Sensitivity analysis

The LCOH and its individual contributions are shown in Figure 12 for changes of hourly COP of the thermodynamic model. The LCOH changed by −11 % and 17 %, while the COP was changed by ±20 % for each hour. As shown, the COP has an effect on the electricity costs, the associated taxes and the tariffs only. The piping costs to access the seawater were also affected, because a change in COP required different volume flow rates of the heat source and consequently smaller or larger pipe diameters. The investment costs of the HP and the storage as well as the maintenance costs remained unchanged. Therefore, the effect on the LCOH due to changes in COP may be limited.

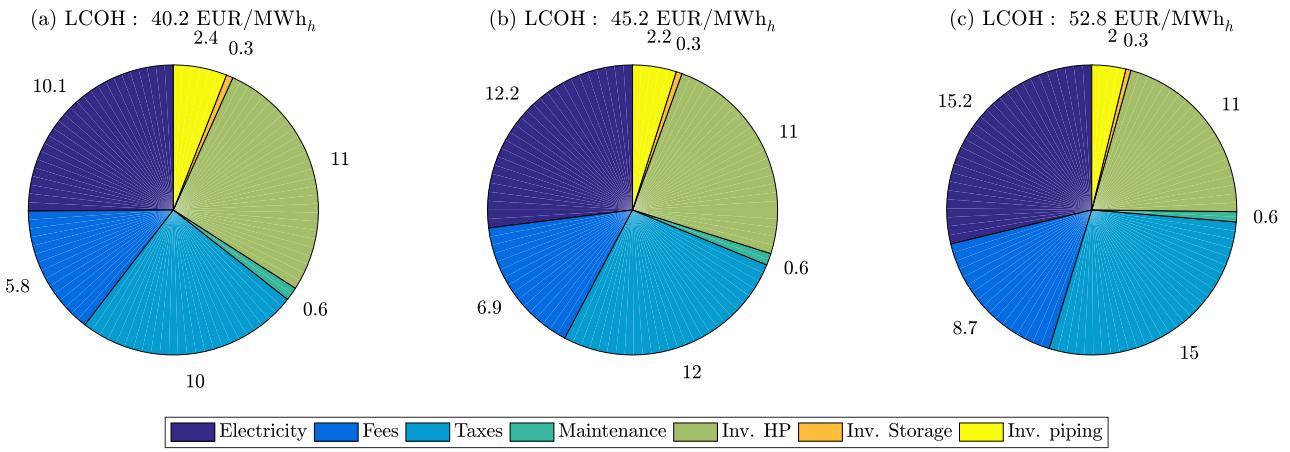

Figure 12. LCOH for optimization based on thermodynamic HP model with −20 % COP_m (a), COP_m (b) and +20 % COP_m (c)

The results of the optimization when varying input parameters of the different COP estimation methods are shown in Table 8.

Table 8. Results of sensitivity analysis

Parameter	−20 % COP_{con}	+20 % COP_{con}	−20 % η_L	η_L=0.5	-20 % c_J	+20 % c_J
Heat source	Sea/GW	Sea/GW	Sea/Air	Sew	Sea/GW	Sea/GW
HP capacity, MW	10.4/5.0	10.4/5.0	11.9/3.8	16.4	10.4/5.0	10.4/5.0
Storage, MW	30.0	33.2	28.8	32.7	32.2	31.6
Seasonal COP, -	2.6	4.0	2.9	3.4	3.5	3.2
LCOH, €/MWh$_h$	55.2	41.6	51.3	47.4	45.1	47.9
Electricity, O&M, €/MWh$_h$	41.3	27.5	37.4	32.4	31.1	33.9
Emissions, kgCO_2/MWh$_h$	86.2	56.9	80.5	68.9	65.1	71.0

As shown for the constant COP, the most economical heat source and HP capacity remained unchanged for variations of ±20 %. However, the SCOPs changed considerably and therefore also the costs for electricity and consequently the LCOH. For a SCOP of 2.6 and 4.0, the LCOH changed by 18 % and −11 %, respectively. Such a difference may have a significant impact on the decision of investing into HPs compared to alternative supply options and in which heat source. In addition, the impact on the calculated CO_2 emissions is very large with differences of 19.2 kgCO_2/MWh$_h$ and 10.1 kgCO_2/MWh$_h$ for lower and higher assumed COPs, respectively.

With a decreased Lorenz efficiency, the optimal solution was a 11.9 MW seawater HP and a 3.8 MW air-source HP, which was different than the initial found optimum using this method. If the Lorenz efficiency was assumed 0.5 for all HPs, the most economical solution would look again quite different and be based on a large sewage water HP. The deviations in CO_2 emissions are large, when the efficiency is reduced by 20 %.

If the coefficients used for the approximations of the Jensen et al. method were varied by ±20 %, the optimal choice of heat source would switch from seawater to a mix of seawater and groundwater. The deviations in SCOP were smaller than for the sensitivity analysis of the other estimation methods. This would result in similar economic parameters as before. Also, the deviation in CO_2 emissions is small compared to the ones based on the other estimations. Consequently, the results when using the Jensen et al. method may be less sensitive to a wrong choice of input parameters than the ones based on the other methods.

4. Discussion

The aim of the study was to investigate how well different COP estimation methods represent HP performance and how their implementation in an energy planning tool would affect the optimization results. Therefore, the most economical solution found should be seen as an indication. A detailed sensitivity analysis on the economic input parameters was not performed.

The economic optimum was flat, so that different combinations of HP capacities and heat sources could result in a solution close to the optimum. This may be seen by the different optimal choices of heat source depending on the used estimation method and the performed sensitivity analysis.

The piping costs may have a significant impact, as shown in Figure 12 for the seawater HP. Therefore, a sewage water HP was not selected as the most economical solution, even though the SCOP was the highest. Using sewage water required a 2 km long pipe. Furthermore, a heat loss of 5 % was added. If sewage water could be accessed without additional piping, investment costs could be reduced. Furthermore, the heat loss would be avoided resulting in lower operating costs. This would decrease the LCOH by around 5 €/MWh$_h$ [56]. Examples of a 10 MW and a 40 MW sewage water HP installation exist in Kalundborg, Denmark [23] and in Malmo, Sweden [57], respectively.

Part-load operation of the HPs was not represented in the energy planning model, the COP estimation methods and therefore also not in the thermodynamic model. Auxiliary electricity consumption for powering fans or pumps was not considered.

Other COP estimation methods were not applied due to the lack of coefficients for the required temperature range, e.g. [17]. The thermodynamic model was of a two-stage HP with open intercooler and ammonia as refrigerant. A polynomial for screw compressors was applied to represent losses due to a mismatch in pressure ratio. Therefore, the results may be limited to these kinds of applications and could be different for others. The deviations of COP were compared to the thermodynamic model, which may calculate different COPs than a real plant. The chosen constant COPs and efficiencies were based on the design conditions of the thermodynamic model. Deviations in COP and the economic solution would be even larger, if less optimal guesses were made, as was shown in the sensitivity analysis.

The considered dead state temperature did not differ considerably from the logarithmic mean temperature of the heat source, $\overline{T}_C$, because it was chosen to be the heat source inlet temperature. Furthermore, the temperature difference between heat source inlet and outlet was assumed to be 5 K. Therefore, the exergy efficiency and Lorenz efficiency were very similar.

Jensen et al. [19] showed that the Lorenz efficiency decreases for an decrease in temperature lift between the hot and the cold stream for constant component characteristics. This may explain the larger deviation in COP in Figure 11 during summer for the Lorenz method, but also for the other estimation methods. During this period, the DH supply temperature decreased by 20 K and most of the heat source temperatures increased by 10 to 20 K. Considering this dependency in the estimation methods may improve the results.

5. Conclusion

The hourly COPs based on four different estimation methods were compared to the COPs calculated by a thermodynamic HP model for four heat sources for one year. The COPs were used in an energy planning tool to investigate the impact of using different COP estimation methods on the most economical solution for a new development district.

It was found that using a constant COP based on design conditions underestimated the COP considerably if the operating conditions are very different to the design conditions. This was the case especially in summer and if ambient air was used as heat source. The economic parameters, obtained using a constant COP, were very dependent on the choice of constant COP. If the constant COP was chosen less optimally, the economic parameters changed considerably.

Using a constant Lorenz efficiency resulted in large deviations in COP when comparing the estimated COP with the COP obtained from the thermodynamic model of up to 60 % in summer, when ambient air was used. Deviations of 20 % were seen for using sewage water and seawater. Consequently, ambient air played an important role for the economic optimum. If the Lorenz efficiency was assumed to be 0.5 for all HPs, the optimum HP capacity was based on sewage water.

Using a constant exergy efficiency resulted in similar deviations as for the case of assuming a constant Lorenz efficiency.

Using the Jensen et al. COP estimation method for design conditions resulted in good COP approximations with deviations of less than 10 % in summer and, for the water-based HPs, less than 2 % in winter.

Using the Jensen et al. method in the energy planning tool resulted in solutions very close to the ones obtained using COPs from the thermodynamic model. Furthermore, the Jensen et al. method was less sensitive to uncertainties in input parameters than the other estimation methods. Using a constant COP, a constant exergy or a constant Lorenz efficiency can result in wrong investment decisions if wrong assumptions on COP and efficiencies are made. In addition, the calculated CO_2 emissions with these three methods would deviate considerably from the ones considering the thermodynamic HP model.

Acknowledgments

This research project was funded by EUDP (Energy Technology Development and Demonstration). Project title: ”EnergyLab Nordhavn - New Urban Energy Infrastructures”, project number: 64014-0555.

Nomenclature

C cost, €

c coefficients for approximations, -

COP coefficient of performance, -

c_p specific heat capacity, MJ/kg/K

$\dot{E}$ exergy rate, MWh/h

f_{loss} heat loss factor, %

f_Q compressor heat loss ratio, -

LCOH levelized cost of heat, €/MWh

$\dot{m}$ mass flow rate, kg/s

P electricity consumption, MWh

p pressure, bar

Q heat, MWh

$\dot{Q}$ heat rate, MWh/h

s specific entropy, MJ/kg

SCOP seasonal coefficient of performance, -

$\bar{T}$ logarithmic mean temperature, K

T temperature, °C or K

UA overall heat transfer coefficient times area, kW/K

v built-in volume ratio, -

$\dot{W}$ power, MWh/h

w work, MJ/kg

Z objective function, €

Greek symbols

Δ difference
ε exergy efficiency, -
η efficiency, -
κ polytrophic exponent, -
π built-in pressure ratio, -

Subscripts and superscripts

0 dead state
a annualised
b discount rate
amb ambient
C heat source
c compression
con constant
char charging
d design conditions
dis discharging
e expansion
el electricity
F fuel
H heat sink
Heat heat supply
HP high pressure
i inlet
Inv investment
is isentropic
J Jensen
j stream
L Lorenz
level storage level
LP low pressure
m thermodynamic HP model
max maximum
N hours of a year
n current hour of the year
o outlet
O&M operating and maintenance
P product
p production unit
pp pinch point
r refrigerant

st storage

T lifetime

tot total

References

[1] Lund H, Mathiesen BV, Connolly D, Østergaard PA. Renewable energy systems - A smart energy systems approach to the choice and modelling of 100 % renewable solutions. Chem Eng Trans 2014;39:1–6. doi:10.3303/CET1439001.

[2] Connolly D, Lund H, Mathiesen, Brian Vad Østergaard, Poul Alberg Møller B, Nielsen S, Skov IR, Hvelplund FK, et al. Smart Energy Systems: Holistic and Integrated Energy Systems for the era of 100% Renewable Energy 2013. http://vbn.aau.dk/en/publications/smart-energy-systems(ea354fdf-b1aa-46e0-8bd7-349695be9205).html.

[3] Danish Energy Agency. Energy scenarios for 2020, 2035 and 2050 (Danish) 2014. https://www.energyplan.eu/danish-energy-agency-energy-stategy-2050-100-renewable-energy-scenarios/.

[4] Mathiesen BV, Lund H, Hansen K, Ridjan I, Djørup SR, Nielsen S, et al. IDA' s Energy Vision 2050: A Smart Energy System strategy for 100% renewable Denmark 2015. https://vbn.aau.dk/ws/portalfiles/portal/222230514/Main_Report_IDAs_Energy_Vision_2050.pdf.

[5] PlanEnergi. Overview of large-scale electric (and gas) driven heat pumps, which produce heat for Danish district heating (Danish) 2019. http://planenergi.dk/wp-content/uploads/2019/10/Oversigt-over-store-varmepumper-okt-2019-Dansk-CC.pdf (accessed November 13, 2019).

[6] Lund R, Ilic DD, Trygg L. Socioeconomic potential for introducing large-scale heat pumps in district heating in Denmark. J Clean Prod 2016;139:219–29. doi:10.1016/j.jclepro.2016.07.135.

[7] Department of Development and Planning AU. EnergyPLAN n.d. http://www.energyplan.eu/ (accessed January 26, 2018).

[8] Henning D a G. MODEST—An energy-system optimisation model applicable to local utilities and countries. Energy 1997;22:1135–50. doi:10.1016/S0360-5442(97)00052-2.

[9] Hedegaard K, Balyk O. Energy system investment model incorporating heat pumps with thermal storage in buildings and buffer tanks. Energy 2013;63:356–65. doi:10.1016/j.energy.2013.09.061.

[10] Rinne S, Syri S. Heat pumps versus combined heat and power production as CO2 reduction measures in Finland. Energy 2013;57:308–18. doi:10.1016/j.energy.2013.05.033.

[11] Luickx PJ, Peeters LF, Helsen LM, D'haeseleer WD. Influence of massive heat-pump introduction on the electricity- generation mix and the GHG effect - Belgian case study. Int J Energy Res 2008;32:57–67. doi:10.1002/er.1366.

[12] Mathiesen BV, Lund H. Comparative analyses of seven technologies to facilitate the integration of fluctuating renewable energy sources. IET Renew Power Gener 2009;3:190–204. doi:10.1049/iet-rpg:20080049.

[13] Lund R, Østergaard DS, Yang X, Mathiesen BV. Comparison of Low-temperature District Heating Concepts in a Long-Term Energy System Perspective. Int J Sustain Energy Plan Manag 2017;12:5–18. doi:10.5278/ijsepm.2017.12.2.

[14] Østergaard PA, Andersen AN. Booster heat pumps and central heat pumps in district heating. Appl Energy 2016. doi:10.1016/j.apenergy.2016.02.144.

[15] EMD International A/S. energyPRO n.d. https://www.emd.dk/energypro/# (accessed January 31, 2018).

[16] Jensen JK, Ommen T, Markussen WB, Elmegaard B. Design of serially connected ammonia-water hybrid absorption-compression heat pumps for district heating with the utilisation of a geothermal heat source. Energy 2017;137:865–77. doi:10.1016/j.energy.2017.03.164.

[17] Oluleye G, Smith R, Jobson M. Modelling and screening heat pump options for the exploitation of low grade waste heat in process sites. Appl Energy 2016;169:267–86. doi:10.1016/j.apenergy.2016.02.015.

[18] Oluleye G, Jiang N, Smith R, Jobson M. A novel screening framework for waste heat utilization technologies. Energy 2017;125:367–81. doi:10.1016/j.energy.2017.02.119.

[19] Jensen JK, Ommen T, Reinholdt L, Markussen WB, Elmegaard B. Heat pump COP, part 2: Generalized COP estimation of heat pump processes. Refrig. Sci. Technol., 2018. doi:10.18462/iir.gl.2018.1386.

[20] Ommen T, Jensen JK, Meesenburg W, Jørgensen PH, Pieper H, Markussen WB, et al. Generalized COP estimation of heat pump processes for operation off the design point of equipment. Proc 25th IIR Int Congr Refrig 2019. doi:10.18462/iir.icr.2019.0648.

[21] F-Chart Software. Engineering Equation Solver n.d. http://www.fchart.com/ees/ (accessed February 13, 2017).

[22] Granryd E, Ekroth I, Lundqvist P, Melinder Å, Palm B, Rohlin P. Refrigerating Engineering Part I. Stockholm: Royal Institute of Technology; 2011.

[23] Danish Energy Agency. Inspirationskatalog for store varmepumpeprojekter i fjernvarmesystemet (English: Inspiration catalogue for large-scale heat pump projects in district heating 2017. https://ens.dk/sites/ens.dk/files/Varme/inspirationskatalog_for_store_varmepumper.pdf.

[24] Bejan A, Tsatsaronis G, Moran MJ. Thermal Design and Optimization. 1996. doi:10.1016/S0140-7007(97)87632-3.

[25] GAMS Development Corp. GAMS n.d. https://www.gams.com/ (accessed August 6, 2017).

[26] IBM. CPLEX Optimizer n.d. https://www.ibm.com/analytics/cplex-optimizer (accessed January 5, 2019).

[27] Pieper H, Masatin V, Volkova A, Ommen T, Elmegaard B, Brix Markussen W. Modelling framework for integration of large-scale heat pumps in district heating using low-temperature heat sources: A case study of Tallinn, Estonia. Int J Sustain Energy Plan Manag 2019;20:67–86. doi:https://doi.org/10.5278/ijsepm.2019.20.6.

[28] Boomsma TK, Meibom P, Juul N. Mathematical programming models for energy system analysis: An introduction 2013:1–45. http://orbit.dtu.dk/en/publications/mathematical-programming-models-for-energy-system-analysis-an-introduction(b78b675d-aba0-4a69-8cbd-c4470bc00681).html.

[29] Pieper H, Ommen T, Buhler F, Lava Paaske B, Elmegaard B, Brix Markussen W. Allocation of investment costs for large-scale heat pumps supplying district heating. Energy Procedia 2018;147:358–67. doi:10.1016/j.egypro.2018.07.104.

[30] Danish Energy Agency, Energinet.dk. Technology Data for Energy Plants - Generation of Electricity and District Heating, Energy Storage and Energy Carrier Generation and Conversion 2015. https://ens.dk/en/our-services/projections-and-models/technology-data.

[31] Energylab Nordhavn. EnergyLab Nordhavn: New Urban Energy Infrastructures and Smart Components 2016. http://www.energylabnordhavn.com/about.html (accessed September 20, 2017).

[32] Google Earth TerraMetrics. Nordhavn area 2019. https://www.google.com/earth/versions/.

[33] HOFOR. Heat demand data for Nordhavn for 2018 2019. https://energydata.dk/.

[34] Pieper H, Ommen T, Elmegaard B, Brix Markussen W. Assessment of a combination of three heat sources for heat pumps to supply district heating. Energy 2019;176:156–70.

doi:10.1016/j.energy.2019.03.165.

[35] HOFOR. Personal communication. Building consumption data for 2017. 2018.

[36] Ommen T, Jensen JK, Markussen WB, Reinholdt L, Elmegaard B. Technical and economic working domains of industrial heat pumps: Part 1 - Single stage vapour compression heat pumps. Int J Refrig 2014;55:168–82. doi:10.1016/j.ijrefrig.2015.02.011.

[37] meteoblue. Hourly weather data for Nordhavn in 2018 2019. https://energydata.dk/.

[38] HOFOR. Groundwater temperature measurements for Flexheat 2018.

[39] PlanEnergi. Personal Communication with Bjarke Lava Paaske 2018.

[40] COWI A/S. Indledende vurdering af hydrogeologiske forhold - Ydre Nordhavn (English: Initial assessment of hydrogeological conditions - Outer Nordhavn) 2015. http://kk.sites.itera.dk/apps/kk_annoncering/file.php?f=867.

[41] Ayub Z. World's Largest Ammonia Heat Pump (14 MWh) for District Heating in Norway—A Case Study. Heat Transf Eng 2016. doi:10.1080/01457632.2015.1052716.

[42] Friotherm AG. Värtan Ropsten – The largest sea water heat pump facility worldwide , with 6 Unitop ® 50FY and 180 MW total capacity n.d. http://www.friotherm.com/webautor-data/41/vaertan_e008_uk.pdf.

[43] Ministry of Environment and Food of Denmark. The Danish Environmental Protection Agency n.d. http://eng.mst.dk/ (accessed January 15, 2018).

[44] HOFOR. Measurements of temperature and volume flow rate for Lynetten sewage water treatment plant 2019.

[45] AS Tallinna Vesi. Personal Communication with Mattias Müür 2018.

[46] Nord Pool. Historical Market Data n.d. https://www.nordpoolgroup.com/historical-market-data/ (accessed January 20, 2019).

[47] Danish Energy. Elforsyningens nettariffer & priser (In English: Electricity supply system tariffs and prices) 2018. https://www.danskenergi.dk/udgivelser/elforsyningens-nettariffer-priser-pr-1-januar-2018.

[48] Danish Energy Agency. Current PSO tariff (In Danish) n.d. https://ens.dk/service/statistik-data-noegletal-og-kort/aktuel-pso-tarif (accessed February 6, 2019).

[49] Danish Energy Agency. Drejebog til store varmepumpeprojekter i fjernvarmesystemet (English: Guide for large-scale heat pump projects in district heating systems) 2017. https://ens.dk/sites/ens.dk/files/Varme/drejebog_for_store_varmepumper.pdf.

[50] Danish Energy Agency. Technology Data for Energy Plants Updated chapters, August 2016 2016:183. https://ens.dk/en/our-services/projections-and-models/technology-data.

[51] Energinet.dk. Current tariffs (In Danish) n.d. https://energinet.dk/El/Tariffer (accessed January 24, 2019).

[52] Dansk Energi. Elforsyningens nettariffer & priser 2016:1–69.

[53] Danish Energy Agency. District Heating Assessment Tool (DHAT) 2017. https://ens.dk/en/our-responsibilities/global-cooperation/district-heating-assessment-tool-dhat (accessed January 15, 2019).

[54] Danish Energy Agency, Energinet.dk. Technology Data for Energy Plants - Generation of Electricity and District Heating, Energy Storage and Energy Carrier Generation and Conversion 2015. doi:ISBN: 978-87-7844-940-5.

[55] Energinet. CO2 Emission Data 2018. https://www.energidataservice.dk/dataset/co2emis/resource_extract/b5a8e0bc-44af-49d7-bb57-8f968f96932d (accessed February 10, 2019).

[56] Pieper H. Characteristics of natural heat sources for heat pumps and their impact in energy planning. 6th Int Symp Adv Refrig Heat Pump Technol 2019.

https://orbit.dtu.dk/en/publications/køle-og-varmepumpeforum-2019-dansk-køledag-2019-amp-6th-internati.

[57] Hoffman K. Large scale heat pumps for high efficiency district heating projects. IOR 2018. https://ior.org.uk/about/sirach/sirach-past-events.